Aspects of the Reaction Mechanism of Ethane Combustion. 2. Nature of the Intramolecular Hydrogen Transfer

Geoffrey E. Quelch,[†,§] Mary M. Gallo,[†,⊥] Mingzuo Shen,[†] Yaoming Xie,[†] Henry F. Schaefer III,[*,†] and David Moncrieff[‡,∥]

Contribution from the Center for Computational Quantum Chemistry, University of Georgia, Athens, Georgia 30602-2556, and Supercomputer Computations Research Institute, B-186, Florida State University, Tallahassee, Florida 32306-4032

Received October 15, 1993. Revised Manuscript Received March 14, 1994[⊗]

Abstract: A detailed molecular understanding of hydrocarbon combustion processes is recognized as an important goal. The specific system studied (via ab initio theoretical methods) in this work is the reaction between the ethyl radical ($CH_3CH_2^{\bullet}$) and molecular oxygen (O_2). Theoretical methods used include restricted open-shell Hartree–Fock (ROHF), configuration interaction including single and double excitations (CISD), coupled cluster including single and double excitations (CCSD), and a perturbational treatment of connected triple excitations [CCSD(T)]. Basis sets up to double-ζ plus polarization (DZP) quality were used. Theoretical results indicate that there are two distinct but energetically proximate intramolecular hydrogen-transfer transition states on the potential energy surface. One of the structures corresponds to a $^2A''$ electronic state (C_s symmetry), the other to a ^2A electronic state (no symmetry); this latter structure is derived from a $^2A'$ planar structure at which the energy Hessian possesses two imaginary vibrational frequencies. At the best level of theory used, DZP CCSD(T) including zero-point vibrational energy corrections, the $^2A''$ transition state lies 4.5 kcal mol^{-1} above the reactants ($CH_3CH_2 + O_2$).

I. Introduction

A detailed discussion of the importance and relevance of ethane combustion reactions has been given in the earlier paper in this series;[1] the latter work will be called paper 1 hereafter. Early research on the mechanism of ethane combustion was reported[2-16] in the 1960s. The possibility of intramolecular hydrogen transfer in alkylperoxy radicals, which may be denoted as ROO$^{\bullet}$, where R is an alkyl moiety, was discussed and at that time generally neglected. However, intramolecular transition states, even if energetically disfavored compared to intermolecular ones, are important since the entropy changes accompanying reactions governed by such mechanisms are ordinarily smaller. In one of the important papers on the fundamentals of alkane combustion, Knox[4] stated that the main debate was whether the reaction proceeded directly from alkyl radical to alkene or via some intramolecular hydrogen transfer. In a related paper, Fish[6] reasoned that the major products of the oxidation reactions of alkanes derived from competing pyrolyses of alkylperoxy radicals.

Since then it has been suspected that transition states for intramolecular hydrogen transfer might by cyclic or "ringlike". In this context, six-membered ring systems have been assumed[5,6] to have no strain energy, five- and seven-membered rings may possess ~7 kcal mol^{-1} of strain energy, and four- and three-membered rings incorporate ~28 kcal mol^{-1} of strain energy. Therefore, hydrogen transfers from γ-C (via a six-membered ring transition state) will occur readily, from β-C (via a five-membered ring transition state) much more slowly, and from α-C (via a four-membered ring transition state) negligibly. Knox suggested that the activation energy for intramolecular hydrogen transfers will be greater than that for intermolecular hydrogen transfers and thus suggested a preference for five-membered or larger ring transition states. Intermolecular hydrogen transfer in the oxidation of *n*-heptane is at most half as fast as intramolecular transfer. Since the Arrhenius preexponential factor for the comparable intramolecular hydrogen transfer must be 2–4 orders of magnitude greater than that for intermolecular transfer, the activation energy for intramolecular hydrogen transfers must be correspondingly higher.

In the first direct experimental work related to the reaction

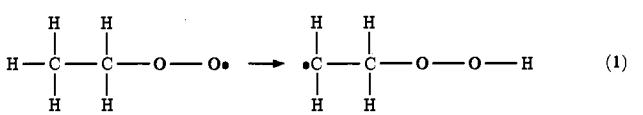

(1)

Baldwin, Pickering, and Walker[7b] determined in 1980 the Arrhenius factor A_1 to be $10^{13.3\pm0.60}$ s^{-1}, the activation energy E_1 to be 34.3 ± 2.4 kcal mol^{-1}, and hence the rate constant k_1 to be 1.95×10^3 s^{-1} at 480 °C. This is close to previous determinations of k for a 1,4 hydrogen transfer (i.e., 2.2×10^3 s^{-1}) in the $CH_3CH_2CH_2CH_2OO$ radical at the same temperature.

† University of Georgia.
‡ Florida State University.
§ Present address: Department of Chemistry, P.O. Box 7486, Wake Forest University, Winston-Salem, NC 27109.
⊥ Present address: BIOSYM Technologies Inc., 10065 Barnes Canyon Rd., San Diego, CA 92121.
∥ Present address: Kendall Square Research Inc., 170 Tracer Lane, Waltham, MA 02154-1379.
⊗ Abstract published in *Advance ACS Abstracts,* May 1, 1994.
(1) Quelch, G. E.; Gallo, M. M.; Schaefer, H. F. *J. Am. Chem. Soc.* **1992**, *114*, 8239.
(2) Benson, S. W. *J. Chem. Phys.* **1961**, *37*, 2662.
(3) Fish, A. *Q. Rev. Chem. Soc., London* **1964**, *18*, 243.
(4) Knox, J. H. *Combust. Flame* **1965**, *9*, 297.
(5) Benson, S. W. *J. Am. Chem. Soc.* **1965**, *87*, 972.
(6) Fish, A. *Angew. Chem., Int. Ed. Engl.* **1968**, *7*, 45.
(7) (a) Baker, R. R.; Baldwin, R. R.; Walker, R. W. *J. Chem. Soc., Faraday Trans. 1* **1975**, *71*, 736, 756. (b) Baldwin, R. R.; Pickering, I. A.; Walker, R. W. *J. Chem. Soc., Faraday Trans. 1* **1980**, *76*, 2374.
(8) Baldwin, R. R.; Higham, M. W. M.; Walker, R. W. *J. Chem. Soc., Faraday Trans. 1* **1972**, *76*, 1615.
(9) Rao, C. N. R.; Kulkarmi, G. V.; Rao, A. M.; Singh, U. C. *J. Mol. Struct. (THEOCHEM)* **1984**, *113*, 113.
(10) (a) Slagle, I. R.; Feng, Q.; Gutman, D. *J. Phys. Chem.* **1984**, *88*, 3648. (b) Personal communications from David Gutman to H.F.S. (c) Slagle, I. R.; Ratajczak, E.; Gutman, D. *J. Phys. Chem.* **1986**, *90*, 402.
(11) Baldwin, R. R.; Dean, C. E.; Walker, R. W. *J. Chem. Soc., Faraday Trans. 2* **1986**, *82*, 1445.
(12) McAdam, K. G.; Walker, R. W. *J. Chem. Soc., Faraday Trans. 2* **1987**, *83*, 1509.
(13) Skancke, A.; Skancke, P. N. *J. Mol. Struct. (THEOCHEM)* **1990**, *207*, 201.
(14) Wagner, A. F.; Slagle, I. R.; Sarzynski, D.; Gutman, D. *J. Phys. Chem.* **1990**, *94*, 1853.
(15) Bozzelli, J. W.; Dean, A. M. *J. Phys. Chem.* **1990**, *94*, 3313.
(16) Walch, S. P.; Dunning, T. H. *J. Chem. Phys.* **1980**, *72*, 3221.

0002-7863/94/1516-4953$04.50/0

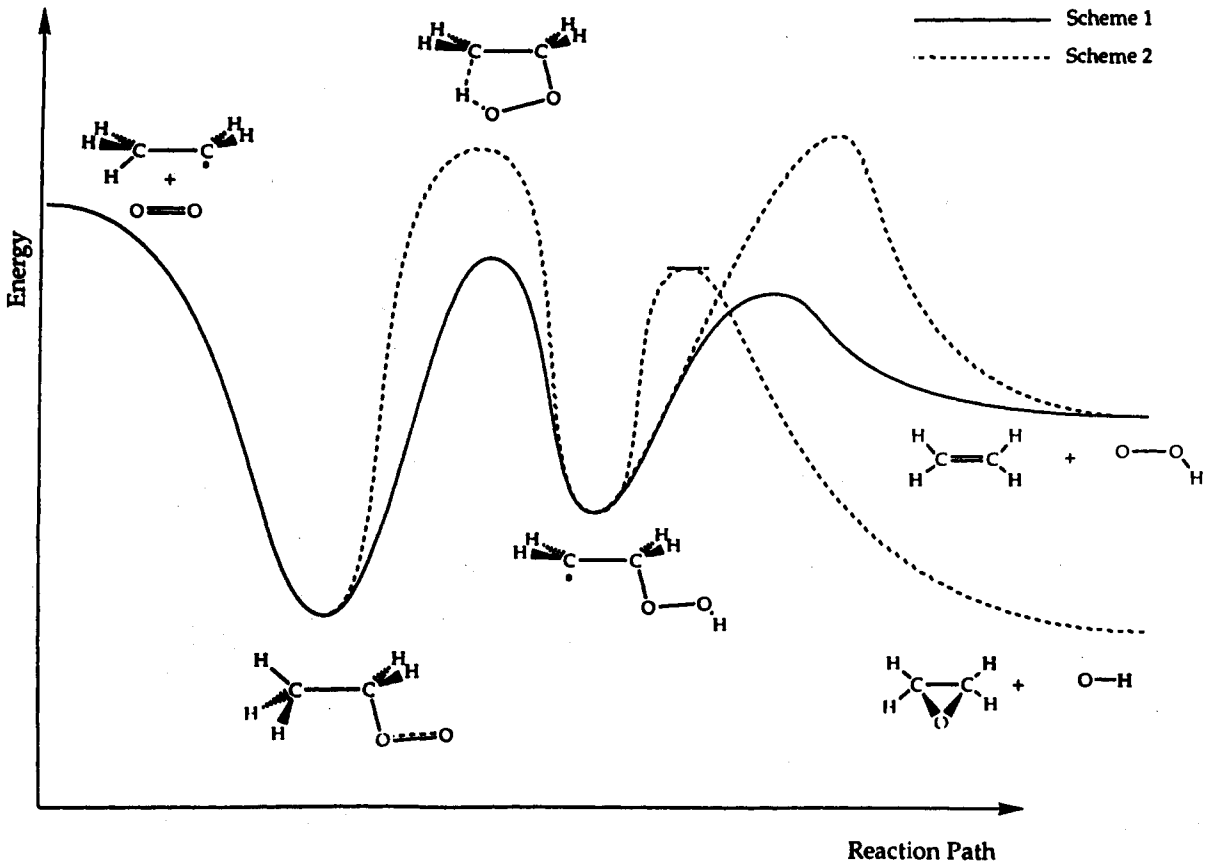

Figure 1. Comparison of experimentally postulated potential energy surfaces for the $CH_3CH_2 + O_2$ reaction. Scheme 1 is that of Slagle, Feng, and Gutman,[10a] while scheme 2 is that of Baldwin, Dean, and Walker.[11] The figure is schematic only. Theoretical relative energies and detailed molecular geometries are presented in the tables, in Figure 2, and in the text.

This value of A_1 is higher than that given by Benson for a 1,5 transfer.[5] In a later (1982) study of the 1,5 intramolecular hydrogen transfer in neopentane, Baldwin, Higham, and Walker[8] determined an Arrhenius factor of 1.20×10^{13} s^{-1} and an activation energy of 28.7 kcal mol^{-1}. These authors argued that the Arrhenius factors should decrease with increasing ring size, since there is a loss of entropy as additional internal rotations are restricted. The difference in activation energy for the intramolecular hydrogen transfer in neopentane (a 1,5 transfer) and ethane (a 1,4 transfer) gives an estimate of the strain energy in a five-membered ring, namely a value of about 6 kcal mol^{-1}.

Slagle, Feng, and Gutman[10] in their 1984 paper discussed their kinetic experimental work in terms of two mechanisms, see Figure 1. They concluded that in order to explain their results, the energy of the transition state for (1) should be 5–6 kcal mol^{-1} below the reactants ($CH_3CH_2 + O_2$) and 23 kcal mol^{-1} above the ethylperoxy radical CH_3CH_2OO. The latter barrier is 11 kcal mol^{-1} lower than that determined by Baldwin, Pickering, and Walker.[7b] However,[10b] the work of Slagle et al.[10a] was a kinetics study done before any measurements of the alkyl–O_2 bond energy were made. The Slagle[10a] estimate of the barrier height was derived from information in older classical studies.

The first of two theoretical papers to deal with the five-membered ring transition state also appeared in 1984. Rao, Kulkarmi, Rao, and Singh[9] in a paper dealing with reactions of HO_2 and related species reported a ring structure of $C_2H_5O_2$ which is not bound. They assumed an HO_2 moiety interacting with a CH_2CH_2 molecule and concluded that the $C_2H_5O_2$ ring is not stable with respect to the former species.

In 1986, Baldwin, Dean, and Walker[11] studied the rate of reaction of CH_2CH_2 with HO_2, the reverse of the ethane combustion reaction. Their results showed that it was difficult to explain the high yields of alkenes from the forward (combustion) reaction, due probably to the requisite "highly strained" 1,4 hydrogen transfer in the CH_3CH_2OO radical. These authors suggested that the barrier height devised by Slagle, Feng, and Gutman[10] be increased from 23 to 31 kcal mol^{-1}. This change results in the route from CH_2CH_2OOH to CH_2CH_2 proposed by Slagle et al. being ruled out of the combustion mechanism. These authors therefore conclude that the direct route to CH_2CH_2 formation is more probable, and hence there is no need for the five-membered ring transition state. Additional work in 1987 on this subject by McAdam and Walker[12] suggested that the negative temperature coefficient observed in all major experiments to date was due to a five-membered ring intermediate on the surface, again negating the need for a five-membered ring transition state.

A second theoretical study on the potential energy surface of the $CH_2CH_2 + HO_2$ addition was published by Skancke and Skancke[13] in 1990. Their predictions for the intramolecular hydrogen-transfer transition state show a C_1 structure with an imaginary vibrational frequency of $3312i$ cm^{-1} assigned to the hydrogen-transfer mode. No structures of C_s symmetry were reported. Their work was based on the unrestricted Hartree–Fock (UHF) method, and corrections for spin contamination amounted to 10 kcal mol^{-1} in some cases.

More recent kinetic modeling work[14,15] has suggested that all experimental data can be explained in terms of the reaction scheme devised by Slagle, Feng, and Gutman in 1984. This scheme includes a five-membered ring transition state and is compared with the proposal of Walker in Figure 1. In particular,[10b] in the comprehensive study of the kinetics and the thermochemistry of the reaction $CH_3CH_2 + O_2$ by Wagner, Slagle, Sarzynski, and Gutman,[14] a barrier height (to the intramolecular hydrogen-transfer transition state from the ethylperoxy radical CH_3CH_2-OO) obtained from experiments and modeling, without reliance on information from the classical literature, is 30.5 kcal mol^{-1} at 0 K and 30.2 kcal mol^{-1} at 298 K. These values are closed to what Baldwin et al.[7b] state the barrier height should be.

II. Hydrogen-Transfer Reactions

Hydrogen-transfer reactions are ubiquitous in chemistry and biology. Theoretical studies of many types of hydrogen transfer have been published, and samples are given in the references.[16-28] The work of Dorigo and Houk[25] demonstrates, for the CH_4 + OH reaction, that increasing the distance between the centers of transfer (C and O in this case) by 0.1 Å increases the activation energy by 1.2 kcal mol^{-1}. This increase in activation energy would result in a 7-fold increase in the rate of reaction at 25 °C. However, an increase of 20° in the bond angle whose apex is at the transfering hydrogen is needed to increase the activation energy by 1.0 kcal mol^{-1}. Dorigo and Houk[25] then suggested that for systems where the centers of transfer cannot be less than 2.8 Å apart, other reaction paths, such as intermolecular hydrogen transfer, will predominate. For example, in the CH_4 + OH reaction, constraining the C–O distance to 2.8 Å gives a 9.0 kcal mol^{-1} increase in the activation energy and a decrease in the rate of reaction by a factor of 3×10^6. However, in other work in this area, some systems can show measurable intramolecular hydrogen transfers across center-of-transfer distances greater than 2.8 Å. Thus the rate of hydrogen-transfer reactions is not a simple function of spatial separations between centers of transfer.

III. Theoretical Methods

Ab initio molecular orbital quantum chemical methods are applied to seven molecular/electronic systems of interest to the intramolecular hydrogen transfer in the ethane reaction system. These include three electronic states ($^2A''$, $^2A'$, and ^2A) of a ringlike structure, two of which are transition states. A schematic drawing of this ringlike structure is shown below. See Figure 2 for more realistic molecular geometric

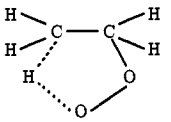

parameters of these three electronic states. The products of the reaction of ethyl radical and oxygen, namely the molecules CH_2CH_2 and HO_2, in

$$CH_3CH_2 + O_2 \rightarrow CH_2CH_2 + HO_2$$

have also been studied in their electronic ground states. Detailed drawings for the products, CH_2CH_2 and HO_2, are omitted. The reactant molecules, CH_3CH_2 and O_2, as well as an intermediate, the ethylperoxy radical CH_3CH_2OO, have been studied at comparable levels of theory previously, as reported in paper 1. A complex between the products, denoted as $CH_2CH_2\cdots HO_2$ or $C_2H_4\cdots HO_2$, is included in this report, as is the hydroperoxyethyl radical, $^{\bullet}CH_2CH_2OOH$. The latter two molecules are intermediates en route from the reactants CH_3CH_2 and O_2 to the products CH_2CH_2 and HO_2. The principal new results here are those for the three electronic states of the ringlike structure, in particular the two transition states. See Figure 1, which is a summary of two experimentally proposed reaction mechanisms, for an overall schematic disposition of the various molecular species mentioned.

Initially the $^2A'$ and $^2A''$ electronic states of the planar five-membered ringlike structure were investigated. The $^2A'$ stationary point possesses two imaginary vibrational frequencies and hence is not a true transition state on the potential energy surface. The mode with a less negative harmonic vibrational frequency was followed into C_1 symmetry and the true transition state (of ^2A symmetry) located. In order to be certain of the nature of the transition states, the intrinsic reaction coordinates (IRCs) emanating from the $^2A''$ and ^2A transition states were determined. The IRCs thus determined link the ethylperoxy radical CH_3CH_2OO, through the transition states, to the intermediates on the other side of the hill on the potential energy surface. Although the IRCs are only models of dynamical reality, they do serve to link reactants and products.

Three Gaussian-type atomic basis sets have been used here. The smallest basis used was the STO-3G set of Hehre, Stewart, and Pople.[29] The second basis was the standard double-ζ (DZ) set of Huzinaga[30] and Dunning,[31] designated C, O (9s5p/4s2p), H (4s/2s). The largest basis was the double-ζ plus polarization (DZP) set, constructed by adding to the DZ basis set a set of six d-like functions to each carbon atom, with orbital exponent $\alpha_d(C) = 0.75$, and to each oxygen atom, $\alpha_d(O) = 0.85$, and a set of p functions to each hydrogen atom, $\alpha_p(H) = 0.75$. The number of basis functions for $C_2H_5O_2$ was therefore 25 for the STO-3G basis, 50 for DZ, and 89 for DZP.

Restricted open-shell Hartree–Fock theory[32a] (ROHF) was initially used for all molecular systems. Optimized stationary points were reached using analytic ROHF energy gradients,[32b] exploiting internal coordinates. Harmonic vibrational frequencies were evaluated at ROHF equilibrium geometries via the use of analytic ROHF energy second derivatives.[32c] Infrared intensities[32d] also were evaluated analytically, within the double harmonic approximation. ROHF zero-point vibrational energies (ZPVEs) were obtained from ROHF harmonic vibrational frequencies scaled by a factor of 0.91, a new value proposed by Grev, Janssen, and Schaefer.[33] All computations except the determination of IRCs were carried out using our own PSI (version 2) computer program system.[34] We have determined IRCs at the DZP ROHF level of theory using GAUSSIAN92.[35] In computing the IRCs, we started with the transition-state structures and analytic Cartesian energy Hessians, used mass-weighted Cartesian coordinates, and stepped into points of the potential energy surface at which the ROHF energy gradients were small.

Effects of electron correlation were taken into account by the use of the configuration interaction with single and double excitations (CISD) method. Geometry optimizations at the CISD level were performed utilizing CISD analytic energy gradients.[36] The Davidson correction for unlinked quadruple excitations in the CISD formulation (denoted by CISD + Q in the text and tables) has also been applied.[37] The active space for all CISD studies included all orbitals except the carbon and oxygen 1s; no virtual orbitals were excluded. The reference function of the CISD is the restricted open-shell Hartree–Fock single determinant. To emphasize this fact, the CI wave function is sometimes written as ROHF–CISD. The largest CISD optimization reported here contained 502 180 configuration-state functions in C_1 symmetry. The harmonic vibrational frequencies at the CISD level were determined by calculating the energy Hessian from finite differences of analytic energy gradients, at displacements from the stationary point along either Cartesian or internal coordinates. The displacements along Cartesian coordinates were 0.01 au long, and the central difference approximations were made (in other words, along each coordinate, both the positive and negative displacements were made). The displacements along the internal

(17) Dunning, T. H.; Walch, S. P.; Goodgame, M. M. *J. Chem. Phys.* **1981**, *74*, 3482.
(18) Schlegel, H. B. *J. Phys. Chem.* **1982**, *86*, 4878.
(19) Ha, T.-K.; Radloff, C.; Nguyen, M. T. *J. Phys. Chem.* **1986**, *90*, 2991.
(20) Wu, Y.-D.; Houk, K. N. *J. Am. Chem. Soc.* **1987**, *109*, 906.
(21) Dorigo, A. E.; Houk, K. N. *J. Am. Chem. Soc.* **1987**, *109*, 2195.
(22) Wu, Y.-D.; Houk, K. N. *J. Am. Chem. Soc.* **1987**, *109*, 2226.
(23) Jensen, F.; Houk, K. N. *J. Am. Chem. Soc.* **1987**, *109*, 3139.
(24) Loncharich, R. J.; Houk, K. N. *J. Am. Chem. Soc.* **1988**, *110*, 2089.
(25) Dorigo, A. E.; Houk, K. N. *J. Org. Chem.* **1988**, *53*, 1650.
(26) Dorigo, A. E.; McCarrick, M. A.; Loncharich, R. J.; Houk, K. N. *J. Am. Chem. Soc.* **1990**, *112*, 7508.
(27) Francisco, J. S. *J. Chem. Soc., Faraday Trans.* **1992**, *88*, 1943.
(28) Francisco, J. S.; Mina-Camilde, N. *Can. J. Chem.* **1993**, *71*, 135.
(29) Hehre, W. J.; Stewart, R. F.; Pople, J. A. *J. Chem. Phys.* **1969**, *51*, 2657.
(30) Huzinaga, S. *J. Chem. Phys.* **1965**, *42*, 1293.
(31) Dunning, T. H. *J. Chem. Phys.* **1970**, *53*, 2823.
(32) (a) The original ROHF wave function was proposed: Roothaan, C. C. J. *Rev. Mod. Phys.* **1960**, *32*, 179. (b) ROHF analytic energy gradient technique used: Goddard, J. D.; Handy, N. C.; Schaefer, H. F. *J. Chem. Phys.* **1979**, *71*, 1525. (c) ROHF analytic energy Hessian technique used: Osamura, Y.; Yamaguchi, Y.; Schaefer, H. F. *Chem. Phys.* **1986**, *103*, 227. (d) ROHF IR intensity technique: Yamaguchi, Y.; Frisch, M. J.; Gaw, J. F.; Schaefer, H. F.; Binkley, J. S. *J. Chem. Phys.* **1986**, *84*, 2262.
(33) Grev, R. S.; Janssen, C. L.; Schaefer, H. F. *J. Chem. Phys.* **1991**, *95*, 5128.
(34) The PSI computer program system is distributed by PSITECH, Inc., Watkinsville, Georgia.
(35) Frisch, M. J.; Trucks, G. W.; Head-Gordon, M.; Gill, P. M. W.; Wong, M. W.; Foresman, J. B.; Johnson, B. G.; Schlegel, H. B.; Robb, M. A.; Replogle, E. S.; Gomperts, R.; Andres, J. L.; Raghavachari, K.; Binkley, J. S.; Gonzalez, C.; Martin, R. L.; Fox, D. J.; Defrees, D. J.; Baker, J.; Stewart, J. J. P.; Pople, J. A. *Gaussian92*, Revision C; Gaussian, Inc.: Pittsburgh, PA, 1992.
(36) (a) Osamura, Y.; Yamaguchi, Y.; Schaefer, H. F. *J. Chem. Phys.* **1981**, *75*, 2919. (b) Osamura, Y.; Yamaguchi, Y.; Schaefer, H. F. *J. Chem. Phys.* **1982**, *77*, 383. (c) Rice, J. E.; Amos, R. D.; Handy, N. C.; Lee, T. J.; Schaefer, H. F. *J. Chem. Phys.* **1986**, *85*, 963.
(37) Langhoff, S. R.; Davidson, E. R. *Int. J. Quantum Chem.* **1974**, *8*, 61.

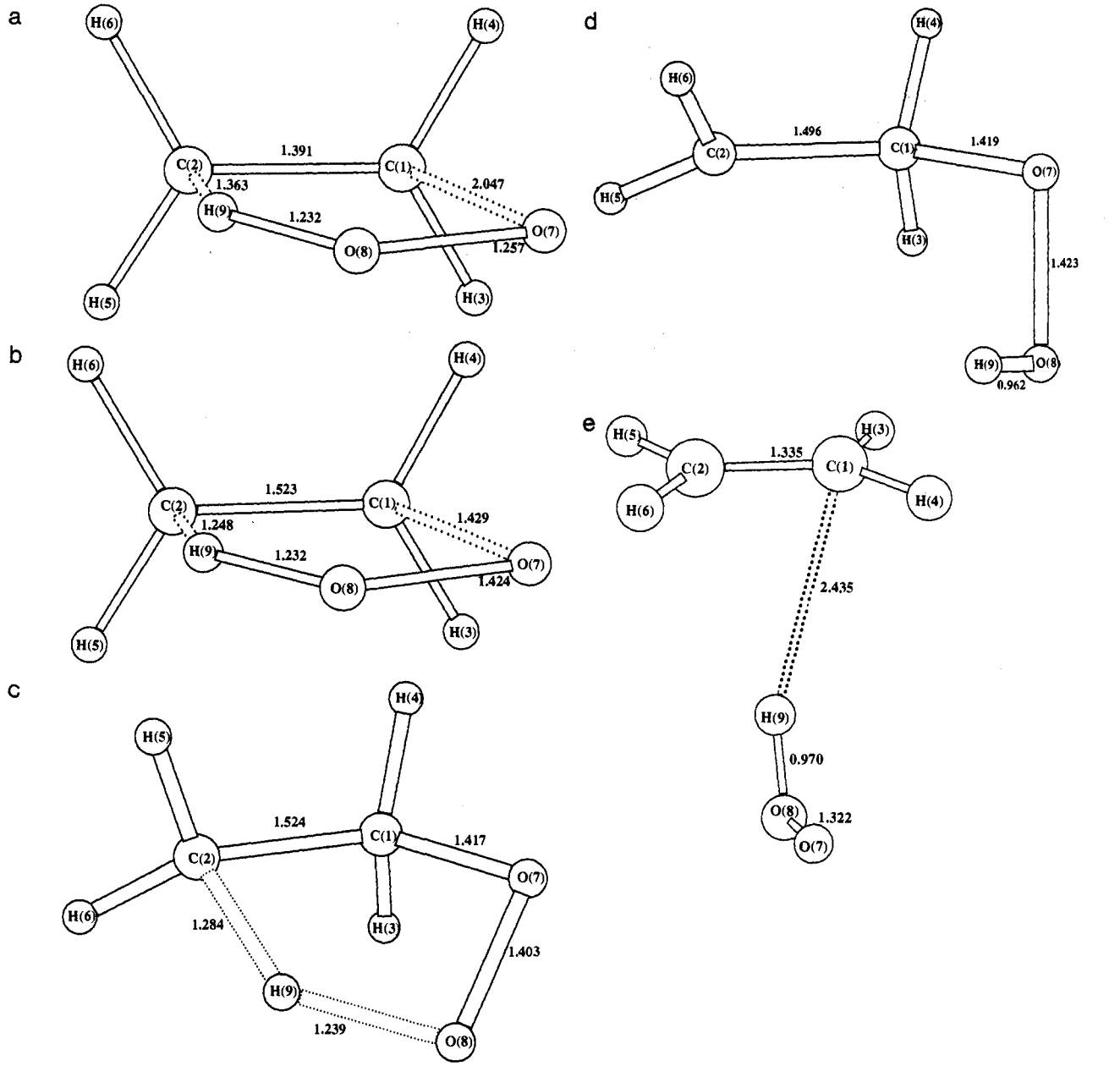

Figure 2. Theoretical (DZP CISD) molecular structures of new molecular/electronic systems discussed in this report. (a) The ringlike $C_2H_5O_2$ $^2A''$ stationary point that is a transition state connecting the ethylperoxy radical CH_3CH_2OO with the complex $CH_2CH_2\cdots HO_2$. Internuclear distances are in angstroms, optimized at the DZP ROHF–CISD level of theory. (b) The ringlike $C_2H_5O_2$ $^2A'$ stationary point that has Hessian index 2. Bond lengths are in angstroms, optimized at the DZP ROHF–CISD level of theory. This stationary point collapses to the C_1 symmetry structure in Figure 2c when the imaginary vibrational frequency of smaller magnitude is followed. (c) The ringlike $C_2H_5O_2$ ^2A stationary point that is a transition state connecting the ethylperoxy radical CH_3CH_2OO with the hydroperoxyethyl radical CH_2CH_2OOH. Internuclear distances are in angstroms, optimized at the DZP ROHF–CISD level of theory. (d) Predicted equilibrium geometry for the hydroperoxyethyl radical $^{\cdot}CH_2CH_2OOH$, belonging to the point group C_1. This structure has Hessian index 0 (local minimum) at the DZP ROHF level of theory. Bond lengths are in angstroms, optimized at the DZP ROHF–CISD level of theory. It appears as the product of the reaction mechanism $CH_3CH_2OO^{\cdot}$ [s,g] $\rightarrow$ $C_2H_5O_2$ (^2A) $\rightarrow$ $^{\cdot}CH_2CH_2OOH$ (C_1). The reactant $CH_3CH_2OO^{\cdot}$ [s,g] is described in ref 1. (e) Predicted equilibrium geometry for the complex $CH_2CH_2\cdots HO_2$ belonging to the point group C_1. This structure has Hessian index 0 (local minimum) at the DZP ROHF level of theory. Bond lengths are in angstroms, optimized at the DZP ROHF–CISD level of theory. It appears in the following reaction mechanism: $CH_3CH_2OO^{\cdot}$ [s,g] $\rightarrow$ $C_2H_5O_2$ ($^2A''$) $\rightarrow$ $CH_2CH_2\cdots HO_2^{\cdot}$ (C_1). The equilibrium structure $CH_3CH_2OO^{\cdot}$ [s,g] is described in ref 1.

coordinates were 0.005 Å for bond lengths and 0.01 rad for bond and torsional angles. Again, for totally symmetric internal coordinates, both positive and negative displacements were made.

Since transition states are often difficult to characterize on a potential energy surface, additional electron correlation energy studies were performed using the coupled cluster method with single and double excitations[38] (CCSD) and CCSD with a perturbational treatment of connected triple excitations [CCSD(T)].[39] All coupled cluster results were obtained at the DZP CISD stationary point geometries. The active space for the CCSD and CCSD(T) wave functions included all orbitals except the carbon and oxygen 1s orbitals and their corresponding virtual orbitals. A single-point DZP CCSD(T) energy computation for a C_1 symmetry molecule with four frozen core and four deleted virtual MOs consumed about 90 CPU hours on the IBM RS6000 Model 580, the fastest model of the second-generation POWER architecture. The CCSD results include the coupled cluster "diagnostic" t_1, which gives an indication of the multireference nature expected for a molecular electronic state.[40]

(38) (a) Scuseria, G. E.; Scheiner, A. C.; Lee, T. J.; Rice, J. E.; Schaefer, H. F. *J. Chem. Phys.* **1986**, *86*, 2881. (b) Scuseria, G. E.; Janssen, C. L.; Schaefer, H. F. *J. Chem. Phys.* **1988**, *89*, 7382.

(39) (a) Scuseria, G. E.; Lee, T. J. *J. Chem. Phys.* **1990**, *93*, 5851. (b) Scuseria, G. E. *Chem. Phys. Lett.* **1991**, *176*, 27.

Table 1. ROHF Theoretical Results: Selected Geometric Parameters (in Å and deg) for the $^2A''$, $^2A'$, and ^2A Electronic States of the Ringlike Structure (Figure 2), the Complex $CH_2CH_2\cdots HO_2$, the Hydroperoxyethyl CH_2CH_2OOH, and the Products CH_2CH_2 and HO_2[a]

	$^2A''$		$^2A'$		^2A		$CH_2CH_2\cdots HO_2$		CH_2CH_2OOH	CH_2CH_2 and HO_2	
	DZ	DZP	DZ	DZP	DZ	DZP	DZ	DZP	DZP	DZ	DZP
r_{12}	1.408	1.397	1.530	1.523	1.529	1.522	1.336	1.327	1.501	1.334	1.324
r_{17}	2.092	2.002	1.466	1.418	1.454	1.406	4.124	3.880	1.413		
r_{78}	1.308	1.244	1.448	1.390	1.444	1.381	1.372	1.312	1.389	1.372	1.312
r_{89}	1.351	1.276	1.193	1.197	1.206	1.211	0.960	0.954	0.948	0.958	0.952
r_{28}	2.543	2.518	2.323	2.285	2.332	2.299	3.564	3.589	2.902		
r_{29}	1.291	1.333	1.324	1.287	1.343	1.312	2.628	2.655	3.022		
θ_{217}	97.5	99.6	106.0	106.3	103.3	103.0	80.7	89.8	113.7		
θ_{178}	101.6	102.8	107.4	108.2	103.8	103.5	56.8	65.7	108.4		
θ_{789}	96.3	96.5	98.7	99.3	96.8	96.7	107.6	105.7	103.1	107.7	105.8
θ_{298}	148.5	149.5	134.6	133.8	132.4	131.3	164.7	166.0	73.7		
γ	1	1	2	2	1	1	0	0	0	0	0

[a] All atomic labels are consistent and are found in Figure 2. r_{ij} is the internuclear distance in angstroms between atoms i and j, and θ_{ijk} is the bond angle in degrees, with j at the apex. γ is the Hessian index, the number of imaginary harmonic vibrational frequencies at each stationary point.

Table 2. ROHF–CISD Theoretical Results: Selected Geometric Parameters (in Å and deg) for the $^2A''$, $^2A'$, and ^2A Electronic States of the Ringlike Structure (Figure 2), the Complex $CH_2CH_2\cdots HO_2$, the Hydroperoxyethyl CH_2CH_2OOH, and the Products CH_2CH_2 and HO_2[a]

	$^2A''$		$^2A'$		^2A		$CH_2CH_2\cdots HO_2$		CH_2CH_2OOH	CH_2CH_2 and HO_2	
	DZ	DZP	DZ	DZP	DZ	DZP	DZ	DZP	DZP	DZ	DZP
r_{12}	1.414	1.391	1.547	1.523	1.547	1.524	1.356	1.335	1.496	1.353	1.333
r_{17}	2.153	2.047	1.496	1.429	1.483	1.417	3.958	4.124	1.419		
r_{78}	1.314	1.257	1.509	1.424	1.496	1.403	1.402	1.322	1.423	1.404	1.324
r_{89}	1.314	1.232	1.233	1.232	1.246	1.239	0.984	0.970	0.962	0.981	0.966
r_{28}	2.558	2.511	2.346	2.287	2.359	2.309	3.421	3.564	2.914		
r_{29}	1.345	1.363	1.302	1.248	1.328	1.284	2.505	2.628	2.909		
θ_{217}	96.9	99.1	106.1	106.5	102.8	102.6	69.3	80.7	113.1		
θ_{178}	100.2	101.0	106.2	107.3	101.8	102.2	59.9	56.8	107.4		
θ_{789}	98.3	97.5	97.7	98.2	95.3	95.0	106.0	107.6	101.7	106.3	104.8
θ_{298}	148.2	150.8	135.3	134.4	132.8	132.4	154.8	164.7	80.8		
γ		1		2		1					

[a] All atomic labels are consistent and are found in Figure 2. r_{ij} is the internuclear distance in angstroms between atoms i and j, and θ_{ijk} is the bond angle in degrees with j at the apex. γ is the Hessian index, the number of imaginary harmonic vibrational frequencies at each stationary point.

IV. Results

The three electronic states of the ringlike structure are shown in Figure 2a–c, where the numerical geometrical parameters were optimized at the DZP CISD level of theory. Notice that the atomic sequential numbers for the ring atoms are the same for all three. IRCs determined at the DZP ROHF level of theory establish that the $^2A''$ transition state links the C_1 [s,g] conformer[1] of the ethylperoxy radical CH_3CH_2OO on one side and a C_1 $CH_2CH_2\cdots HO_2$ on the other side of the saddle point and that the ^2A transition state links the same the C_1 [s,g] conformer[1] of the ethylperoxy radical CH_3CH_2OO on one side and a C_1 hydroperoxyethyl radical CH_2CH_2OOH on the other. The hydroperoxyethyl radical CH_2CH_2OOH, Figure 2d, and the complex $CH_2CH_2\cdots HO_2$, Figure 2e, are labeled in a similar way. The products $CH_2CH_2 + HO_2$ are also fitted into this labeling scheme for simplicity. Selected geometrical parameters of the ROHF-optimized geometries are presented in Table 1 for all seven molecular/electronic systems studied in this research. Likewise, those predicted at the ROHF–CISD level are presented in Table 2. The complete set of internal coordinates is available as supplemental material. γ is called the "Hessian index" and is the number of imaginary harmonic vibrational frequencies for a stationary point at the potential energy surface. Thus, if $\gamma = 0$, then a stationary point is a local minimum on the PES; if $\gamma = 1$, then a stationary point is a transition state. Stationary points where $\gamma > 1$ are sometimes called pointed of "higher Hessian index".

Relative energies of molecular/electronic systems thought to be involved in the reaction $CH_3CH_2 + O_2 \rightarrow CH_2CH_2 + HO_2$ are presented in Table 3. The relative energies include corrections due to the scaled zero-point vibrational energy (ZPVE). The ZPVE is, of course, defined as half the sum of all real harmonic vibrational frequencies:

$$\text{ZPVE} = {}^1/_2 \sum_{i'} \hbar\omega_{i'}$$

where i' runs over normal modes with real harmonic vibrational frequencies only. Harmonic vibrational frequencies determined at the DZP ROHF level of theory were used in determining all ZPVEs, where a scale factor of 0.91 was used, even though DZP CISD harmonic vibrational frequencies are available for some of the cases. This choice is made so that the resulting E_0 are comparable for all molecules/electronic states. Note in Table 3, the symbol "ZPVE(ROHF)" means ZPVE at the DZP ROHF level of theory. Energies for the reactants ($CH_3CH_2 + O_2$) and products ($CH_2CH_2 + HO_2$) at the CISD and CISD+Q levels were obtained by examination of the "supermolecule", i.e., a molecule in which the two moieties at their respective equilibrium geometries are separated by 200 a_0.

Table 4 contains the relative energies of the reactants, products, intermediates, and the two true transition states evaluated at the CCSD and CCSD(T) levels of theory. The ZPVEs at the DZP ROHF level are included in the same manner as in Table 3. The energies in the present table are relative to the reactants and may be compared directly to the Table 3 of Wagner et al.[14] The t_1 diagnostic,[40] obtained as a byproduct in the process of computing the CCSD wave function, is a measure of the "multireference" character of a stationary point and may be used to assess the reliability of single-reference electron correlation methods [such as those used here, CISD, CISD+Q, CCSD, and CCSD(T)] for a given molecular/electronic state. A "large" t_1 value indicates that multireference CI and CC methods should be more appropriate for the particular system in question. There are a few examples of large and small t_1 values in ref 40, and, in comparison, the t_1 values for all molecules/electronic states in Table 4 are relatively small. Therefore, the CISD and CCSD

(40) Lee, T. J.; Rice, J. E.; Scuseria, G. E.; Schaefer, H. F. *Theor. Chim. Acta* **1989**, *75*, 81.

Table 3. Relative Energies (in kcal mol^{-1}) for Molecular/Electronic Systems Thought To Be Involved in the Reaction of Ethyl Radical CH_3CH_2 and Oxygen O_2[a]

E_0[b]	DZ ROHF	DZP ROHF	DZ CISD	DZ CISD+Q	DZP CISD	DZP CISD+Q
$CH_3CH_2 + O_2$[c]	29.4	23.5	31.8	32.6	27.0	28.0
$^2A''$ of [s,g] CH_3CH_2OO[d]	0.0	0.0	0.0	0.0	0.0	0.0
$^2A''$ of $C_2H_5O_2$ (TS)	61.5	61.5	45.4	40.2	46.1	41.3
$^2A'$ of $C_2H_5O_2$	64.5	62.6	49.9	46.4	50.2	46.6
^2A of $C_2H_5O_2$ (TS)	63.2	59.7	48.0	44.5	46.4	42.8
$CH_2CH_2\cdots HO_2$	13.9	15.5	14.2	13.6	19.6	19.3
CH_2CH_2OOH		18.4			17.0	17.4
$CH_2CH_2 + HO_2$[c]	15.8	17.1	16.9	16.3	22.5	22.5
$\Delta H_0°$[e]	−13.6	−6.4	−14.9	−16.3	−4.5	−5.5

[a] All energies are relative to the $^2A''$ state of the [s,g] conformer of ethylperoxy radical CH_3CH_2OO. Included are scaled zero-point vibration energy (ZPVE) corrections as described in the Theoretical Methods section. ROHF-scaled ZPVEs are combined with the CISD and CISD+Q total energies. [b] E_0 is defined as the sum of total energy at the stationary point and the zero-point vibrational energy (ZPVE), where s is a scale factore, chosen to be 0.91 in this report:

$$E_0(\text{ROHF}) = E_e(\text{ROHF}) + s\text{ZPVE(ROHF)}$$

$$E_0(\text{CISD}) = E_e(\text{CISD}) + s\text{ZPVE(ROHF)}$$

$$E_0(\text{CISD+Q}) = E_e(\text{CISD+Q}) + s\text{ZPVE(ROHF)}$$

[c] Supermolecules were used to obtain the CISD and CISD+Q energies. [d] Energies for the ethylperoxy radical CH_3CH_2OO are taken from ref 1. [e] The enthalpy change is for the reaction of our primary interest: $CH_3CH_2 + O_2 \rightarrow CH_2CH_2 + HO_2$. In other words, $\Delta H_0° = E_0(CH_2CH_2 + HO_2) - E_0(CH_3CH_2 + O_2)$.

Table 4. Relative Energies (in kcal mol^{-1}) for the $^2A''$ and ^2A Electronic States of the Ringlike Structure, Reactants ($CH_3CH_2 + O_2$), and Products ($CH_2CH_2 + HO_2$) with DZP CCSD and DZP CCSD(T) Methods Evaluated at the DZP CISD Optimized Geometries[a]

	CISD	CISD+Q	CCSD	CCSD(T)	expt	t_1
reactants	0.0	0.0	0.0	0.0	0.0	
CH_3CH_2 $^2A''$						0.0126
O_2 $^3\Sigma_g^-$						0.0161
CH_3CH_2OO [s,g] ^2A	−27.0	−28.0	−29.5	−30.5	−32.9[b]	0.0281
$C_2H_5O_2$ (TS) $^2A''$	19.1	13.3	10.1	4.5	(−2.4)[c]	0.0319
$C_2H_5O_2$ (TS) ^2A	19.4	14.8	12.4	9.1	(−2.4)[c]	0.0353
CH_2CH_2OOH ^2A	−10.0	−10.6	−9.8	−10.3	−21.9[d]	0.0138
$CH_2CH_2\cdots HO_2$ ^2A	−7.4	−8.7	−11.1	−12.2		0.0258
products	−4.5	−5.5	−7.7	−8.5	−10.8,[e] −13.0[e]	
CH_2CH_2 ^1A_g						0.0103
HO_2 $^2A''$						0.0331

[a] DZP CISD and DZP CISD+Q values are listed for comparison. The values include scaled zero-point vibrational energy corrections as described in the Theoretical Methods section. The t_1 parameter is described in the text. [b] Wagner, Slagle, Sarzynski, and Gutman, ref 14. All enthalpies quoted from this source are for 0 K. The reaction enthalpy −32.9 kcal mol^{-1} is obtained by treating it as a parameter in their theoretical kinetic model, to be varied within the experimentally determined range of Slagle, Ratajczak, and Gutman, ref 10c, to produce optimum agreement between this model and thermochemical and kinetic measurements. [c] Reference 14. The energy difference −2.4 kcal mol^{-1} is obtained by treating it as a parameter in their theoretical kinetic model, to be varied to produce optimum agreement between this model and their wide range of kinetic measurements. [d] Reference 14. The energy difference −21.9 kcal mol^{-1} was an estimate. [e] The value −13.0 kcal mol^{-1} was recommended by Baulch et al., ref 43, for the room temperature (298 K) reaction. The value −10.8 kcal mol^{-1} was determined from heats of formation at 0 K found in Wagman et al., ref 44; therefore, this value may be more directly comparable to our theoretical value of −8.5 kcal mol^{-1}.

methods used here should be accurate for the reactants and products and relatively accurate for the transition states.

In Tables 5 and 7 are presented the harmonic vibrational frequencies and descriptions of the normal modes in terms of internal coordinates for the $^2A''$ and ^2A electronic states of the ringlike structure. The harmonic vibrational frequencies for the $^2A'$ state are briefly listed in Table 6. For atom labels, see Figure 2. As mentioned before in the Theoretical Methods section, harmonic vibrational frequencies were determined from analytic energy Hessians at the ROHF level and from finite differences of analytic energy gradients at the CISD level. All harmonic vibrational frequencies at each level and for each electronic state were determined at their respective stationary points on the potential energy surface. The normal modes are sequentially numbered according to their harmonic vibrational frequency values.

The potential energy distribution (PED) is one way of describing the normal modes in terms of internal coordinates. For example, for the H_2O molecule, if we choose the two bond lengths and the bond angle as internal coordinates, r_{12}, r_{13}, and θ_{213}, then one a_1 mode would have PED r_{12} [50%], r_{13} [50%], and another a_1 mode would have PED θ_{213} [100%]. The b_2 mode of water would have PED r_{12} [50%], r_{13} [−50%]. If we choose the following internal coordinates, $r_{12} + r_{13}$, $r_{12} - r_{13}$, and θ_{213}, then the PEDs are a_1, $r_{12} + r_{13}$ [100%]; a_1, θ_{213} [100%]; and b_2 $r_{12} - r_{13}$ [100%]. Fortunately, in the present case, the "transition vector" (the sole normal mode whose harmonic vibrational frequency is imaginary) cleanly consists of one or two primitive internal coordinates.

The supplementary Tables A–K contain complete geometries, total energies, and harmonic vibrational frequencies for all structures (including products) discussed in this paper.

V. Discussion

(a) Molecular Geometries. The trends of theoretical molecular geometries found for molecules reported in this research are similar to those of paper 1. An increase in basis set at a given level of theory decreases the bond lengths, and addition of electron correlation (from ROHF to ROHF–CISD) increases the bond lengths. Bonds involving oxygen change more than those between carbons; significant new features in this research are the bond lengths and angles involving the migrating hydrogen. The latter two types of bonds are found to have a greater dependence on the level of theory.

For the ethylperoxy radical CH_3CH_2OO in both the $^2A''$ and $^2A'$ states, the C–C bond length is relatively stable between 1.51

Table 5. Theoretical Harmonic Vibrational Frequencies (in cm^{-1}) and Their Descriptions for the $^2A''$ Electronic State of the Ringlike Structure, a Transition State[a]

	irrep	ROHF	ROHF–CISD	PED [DZP ROHF, DZP ROHF–CISD]
1	a''	3442	3394	$r_{13} - r_{14}$ [91, 89%]
2	a''	3362	3346	$r_{25} - r_{26}$ [94, 90%]
3	a'	3345	3293	$r_{13} + r_{14}$ [91, 88%]
4	a'	3275	3250	$r_{25} + r_{26}$ [95, 93%]
5	a'	1807	1753	θ_{892} [51, 52%]; θ_{789} [–49, –47%]
6	a'	1681	1650	θ_{314} [27, 21%]; $\theta_{213} + \theta_{214}$ [–25, –19%]; θ_{789} [23, 30%]
7	a'	1581	1534	θ_{314} [39, 29%]; $\theta_{213} + \theta_{214}$ [–37, –26%]
8	a'	1525	1580	θ_{789} [53, 56%]; θ_{892} [–26, –37%]
9	a''	1456	1387	τ_{1789} [51, 51%]; τ_{2987} [–49, –49%]
10	a'	1352	1359	θ_{789} [39, 41%]; r_{12} [35, 27%]
11	a''	1331	1296	$\theta_{213} - \theta_{214}$ [47, 46%]; τ_{2987} [–24, –26%]; τ_{3178} [–19, –19%]
12	a'	1232	1131	$\theta_{213} + \theta_{214}$ [39, 19%]; θ_{892} [20, 24%]; θ_{789} [–15, –45%]
13	a'	1037	1039	θ_{789} [69, 68%]; θ_{892} [–23, –23%]
14	a''	1034	996	τ_{1789} [61, 60%]; τ_{2987} [–36, –39%]
15	a''	881	866	$\theta_{213} - \theta_{214}$ [44, 46%]; $\tau_{3178} + \tau_{4178}$ [–35, –37%]
16	a'	712	684	θ_{178} [59, 64%]; θ_{789} [–38, –29%]
17	a'	588	571	θ_{178} [79, 72%]; θ_{892} [–9, –27%]
18	a''	562	544	τ_{1789} [50, 49%]; τ_{2987} [–48, –49%]
19	a'	430	455	θ_{892} [40, 39%]; θ_{178} [–26, –17%]; $r_{89} - r_{29}$ [15, 21%]
20	a''	232	294	τ_{1789} [54, 52%]; $\tau_{3178} + \tau_{4178}$ [–45, –47%]
21	a'	2067*i*	1715*i*	$r_{89} - r_{29}$ [45, 40%]; θ_{789} [–39, –43%]

[a] r_{ij} is the bond length between atoms i and j; θ_{ijk} is the bond angle with apex at j; the τ_{ijkl} is the torsional angle viewed along jk. The atom labels are found in Figure 2. Numbers in square brackets are potential energy distributions (PEDs); only the dominant internal coordinates of each normal mode are listed. All frequency values are unscaled. Basis set was DZP.

Table 6. Theoretical (DZP ROHF) Harmonic Vibrational Frequencies for the $^2A'$ Electronic State of the Ringlike Structure[a]

a'	3280, 3227, 1883, 1659, 1588, 1496, 1242, 1202, 1082, 1009, 785, 708, 5731*i*
a''	3369, 3274, 1336, 1266, 1239, 891, 285, 237*i*

[a] Since this electronic state has two imaginary harmonic vibrational frequencies, our interest in it is to follow the mode to a true transition state.

and 1.54 Å. This is in the range of typical carbon–carbon single bonds.[41] For the ringlike structure $C_2H_5O_2$, the ^2A results again show a C–C single bond, but the $^2A''$ state has a significantly shorter C–C bond (1.391 Å) and is thus intermediate between a single (1.54 Å) and a double (1.34 Å) bond in length. The representative C–C double bond length is clearly shown in the products $CH_2CH_2 + HO_2$ and also in the CH_2CH_2···HO_2 complex. Since the $^2A''$ state of ethylperoxy radical CH_3CH_2OO has a C–C single bond and the $^2A''$ state of the ringlike structure $C_2H_5O_2$ has a bond order of approximately 1.5, some significant electronic structure changes must have occurred when the reaction proceeded from $CH_3CH_2 + O_2$ to the $^2A''$ electronic state of the ringlike structure.

We now consider the C_1–O_7 distance in the ringlike $C_2H_5O_2$ structures. The ^2A state shows values (e.g., 1.417 Å for DZP CISD) within the usual range of C–O single bonds. However, the $^2A''$ electronic state of the ringlike $C_2H_5O_2$ shows extremely long C–O internuclear separations, greater than 2.0 Å. Thus the $^2A''$ transition state occurs significantly earlier along the reaction coordinate than does the ^2A transition state. It seems clear that there has been significant redistribution of electron density from the O–O bond to the C–C bond in the $^2A''$ electronic state of the ringlike $C_2H_5O_2$ relative to that in the $^2A''$ state of the ethylperoxy radical CH_3CH_2OO.

(41) Elmsley, J. *The Elements*; Clarendon: Oxford, 1989.

Table 7. Theoretical Harmonic Vibrational Frequencies (in cm^{-1}) and Their Descriptions for the ^2A Electronic State of the Ringlike Structure, a Transition State[a]

	ROHF	ROHF–CISD	PED [DZP ROHF, DZP ROHF–CISD]
1	3367	3338	r_{25} [59, 57%]; r_{26} [–40, –41%]
2	3287	3255	r_{14} [68, 68%]; r_{13} [–23, –26%]
3	3272	3237	r_{26} [57, 57%]; r_{25} [36, 39%]
4	3223	3181	r_{13} [72, 70%]; r_{14} [26, 28%]
5	1900	1866	r_{89} [77, 48%]; θ_{789} [–20, –49%]
6	1636	1579	τ_{3178} [43, 43%]; θ_{314} [35, 34%]; θ_{213} [–16, –17%]
7	1578	1528	θ_{526} [65, 65%]; θ_{621} [–15, –15%]
8	1490	1431	θ_{213} [58, 59%]; τ_{3178} [–32, –32%]
9	1366	1312	θ_{213} [51, 50%]; θ_{214} [–25, –27%]
10	1298	1284	τ_{1789} [38, 61%]; θ_{621} [–23, –13%]; r_{89} [18, 18%]
11	1277	1236	θ_{213} [26, 22%]; τ_{3178} [–21, –21%]; τ_{2178} [16, 20%]
12	1215	1114	r_{17} [29, 44%]; r_{78} [–17, –14%]; τ_{3178} [13, 11%]
13	1187	1167	r_{12} [26, 15%]; θ_{521} [–20, –27%]; τ_{5217} [–18, –16%]
14	1045	977	r_{78} [36, 30%]
15	1019	997	r_{12} [42, 26%]; θ_{521} [18, 22%]
16	946	920	τ_{3178} [46, 47%]; θ_{213} [–26, –27%]
17	745	725	θ_{213} [35, 40%]; τ_{2178} [11, 17%]
18	664	655	r_{89} [39, 21%]; θ_{213} [21, 25%]
19	470	469	τ_{3178} [27, 34%]; τ_{1789} [–23, –20%]; τ_{5217} [22, 17%]; τ_{2178} [18, 22%]
20	292	300	τ_{3178} [50, 47%]; τ_{2178} [44, 47%]
21	5981*i*	4788*i*	r_{89} [100, 99%]

[a] r_{ij} is the bond length between atoms i and j; θ_{ijk} is the bond angle with apex at j; the τ_{ijkl} is the torsional angle viewed along jk. The atom labels are found in Figure 2. Numbers in square brackets are potential energy distributions (PEDs); only the dominant internal coordinates of each normal mode are listed. All frequency values are unscaled. Basis set was DZP.

For the O–O bond lengths in the $^2A'$ and ^2A stationary points, the theoretical values represent typical O–O single bond lengths, namely 1.4–1.5 Å. However, the O–O bond length in the $^2A''$ state is more than 0.1 Å shorter than that in the ^2A state. This confirms our view that the $^2A''$ transition state occurs earlier along the reaction coordinate. Comparing our results with those of Skancke and Skancke,[13] we see that the geometry of their ^2A transition state at the 6-31G* UHF level matches closely our DZP ROHF results. As expected, the major differences show up in the parameters associated with the migrating hydrogen. For the ^2A DZP ROHF results, we have a C_2–H_9 distance of 1.312 Å, while Skancke and Skancke have 1.371 Å and likewise O_8–H_9 distances of 1.211 and 1.215 Å, respectively. Unfortunately, the C_2–H_9–O_8 angle was not reported by Skancke and Skancke.[13]

Geometrical parameters involved intimately with the hydrogen transfer (O_8–H_9, C_2–H_9, C_2–O_8, and C_2–H_9–O_8) are very important for understanding the nature of the transfer process. Both the O–H and C–H separations are longer (~0.3 Å) than typical bonds. In all cases (except DZ ROHF $^2A'$), the C–H distance is longer than the O–H.

The precise details of the geometry adjacent to the migrating hydrogen atom are clearly important factors in discussing hydrogen transfers. Dorigo and Houk[25] have concluded that a C–O distance greater than 2.8 Å will likely cut off the intramolecular hydrogen-transfer reaction channel. In the results presented here, we have C_2–O_8 distances of between 2.30 (^2A DZP ROHF) and 2.56 Å ($^2A''$ DZ CISD); thus the intramolecular hydrogen transfer is a "reasonable" proposal. The values of C_2–H_9 and O_8–H_9 are in line with previous results, as is the angle C_2–H_9–O_8. As noted by Dorigo and Houk,[25] the rate of reaction is somewhat insensitive to large deviations of the C–H–O angle from the preferred linear arragement. This angle is ~150° (DZP ROHF–CISD) for $^2A''$ and 132° for ^2A. The difference between the two cases will clearly impact the activation energies, although on going from $^2A'$ to ^2A, this angle has actually decreased.

Therefore, there must be more important contributions to differences in activation energies than the angle at the migrating hydrogen.

(b) Harmonic Vibrational Frequencies. The $^2A'$ state of the ringlike structure possesses two imaginary frequencies. The larger of the two has an unrealistically large magnitude and is assigned to the hydrogen-transfer coordinate. The smaller of the two imaginary frequencies ($237i$ cm^{-1} at the DZP ROHF level) has a'' symmetry, indicating the presence of a lower energy stationary point in C_1 symmetry. For the $^2A''$ ringlike stationary point (Table 5 and Figure 2a), there is one imaginary vibrational frequency, and thus this system is a true transition state. The imaginary frequency is again assigned to the intramolecular hydrogen transfer with, in this case, a more plausible magnitude ($2067i$ cm^{-1} at the DZP ROHF level and $1715i$ at the DZP CISD level). The basis for this assignment is the potential energy distribution (PED) of the transition vector, about +40% of ($r_{89} - r_{29}$) and –40% of θ_{789}. The C–O bond length r_{17} is much less prominently involved in the transition vector. The ^2A state (Table 7 and Figure 2c) results from the $^2A'$ state. The one imaginary vibrational frequency is again assigned to the intramolecular hydrogen transfer. This assignment is based on the remarkable PED of nearly 100% r_{89}. At the transition state at least, the C···H distance r_{29} contributes little to the transition vector.

The ROHF imaginary vibrational frequency ω_{21} for the $^2A'$ and ^2A electronic states has a unrealistically large magnitude (>5000 cm^{-1} with the three basis sets STO-3G, DZ, and DZP), with the magnitudes for the ^2A electronic state being larger than those for $^2A'$. The value of an imaginary vibrational frequency of a transition state can be thought of as a measure of the "sharpness" of the potential barrier. A magnitude greater than 5000 cm^{-1} is surely an indicator of a breakdown in the theoretical model or of some form of symmetry breaking. The results for this transition state from Skancke and Skancke[13] at the 6-31G* UHF level show a value for ω_{21} of $3316i$ cm^{-1}, which is closer to what one would expect for an imaginary frequency mode of this type. In fact, all the other frequencies are in good agreement (DZP ROHF vs 6-31G* UHF), indicating one difference in the potential energy surfaces for the UHF and ROHF methods. However, large spin contaminations are indicated in the UHF results. At the CISD level of theory, the magnitude of the transition vector frequency is smaller, 4788 cm^{-1}, but still unreasonable.

In the RRKM work of Wagner, Slagle, Sarzynski, and Gutman,[14] a number of assumptions were made for the ring frequencies in the transition state. The most important value is clearly the imaginary frequency (the value for the hydrogen transfer), which was assumed to be $1638i$ cm^{-1}. Our results show a much larger value for this quantity for the $^2A'$ and ^2A states. It is seems clear, however, that this particular symmetry-breaking contaminated result is less reliable than the ad hoc assumptions of Wagner et al. One difficult number to predict, the δ(CHO) motion, was allowed to vary in the RRKM work, the final value being 160 cm^{-1}. Our theoretical studies predict this value to be 285 ($^2A'$), 430 ($^2A''$) and 1019 cm^{-1} (^2A). It must be stressed that these vibrational modes are heavily mixed.

The presence of three stationary points (albeit only two of which possess one imaginary vibrational frequency) for this hydrogen-transfer process suggests that the potential energy surface in the vicinity of the transition state will be very interesting. Clearly, at all levels of theory used to date, there are two energetically close transition states on the hydrogen-transfer potential energy surface. Which transition state the system traverses will depend on the available energy and the precise geometry of the entrance channel. The geometries of the $^2A''$ and ^2A ringlike transition states are very different, and a DZP ROHF IRC study shows that the two transition states link different intermediate products:

$$CH_3CH_2OO\ [s,g] \rightarrow \begin{cases} C_2H_5O_2\ [^2A''] \rightarrow CH_2CH_2...HO_2\ (C_1) \\ C_2H_5O_2\ [^2A] \rightarrow CH_2CH_2OOH\ (C_1) \end{cases}$$

If the ethylperoxy progenitor is of C_s symmetry, a further point of interest arises. Such a structure, on moving toward the hydrogen-transfer point, will reach a bifurcation point on the surface, leading to two different (but energetically degenerate) ^2A structures or to the $^2A''$ structure.

(c) Energetics and Implications for Kinetic Modeling. Relative energies for all species studied here are given in Tables 3 and 4. Energies given in Table 3 were determined at the respectively optimized geometries (ROHF and CISD) and include ZPVEs at DZ or DZP ROHF levels, all relative to the [s,g] conformer of the ^2A ground state of the ethylperoxy radical CH_3CH_2OO (paper 1). Energies given in Table 4 were determined at the respectively optimized DZP CISD geometries, including ZPVE at the DZP ROHF level. Several comparisons of energies are of interest here (see Figure 3 for a more or less scaled diagram of molecular species and energetics).

(i) Consider first the difference between the reactants $CH_3CH_2 + O_2$ and the transition states. Theoretical values between the reactants $CH_3CH_2 + O_2$ and the $^2A''$ transition state are 19.1, 13.3, 10.1, and 4.5 kcal mol^{-1} at the DZP CISD, DZP CISD+Q, DZP CCSD, and DZP CCSD(T) levels of theory, respectively. Theoretical differences between the reactants $CH_3CH_2 + O_2$ and the ^2A transition state are 19.4, 14.8, 12.4, and 9.1 kcal mol^{-1} at similar levels of theory. The ^2A TS always lies above the $^2A''$ TS, and the difference monotonically decreases as the treatment of electron correlation is more complete. Wagner et al.[14] estimated the difference between $CH_3CH_2 + O_2$ and the transition state to be –2.4 kcal mol^{-1}; in other words, Wagner et al. placed the transition state(s) energetically below the reactants. The "theoretical/experimental" value of Wagner et al. was based on their mechanism

$$R + O_2 \rightleftharpoons ROO^* \rightarrow R_{-H}OOH^* \rightarrow R_{-H} + HO_2$$

treating the energetic difference in question as a parameter to be varied in their kinetic modeling, such that the final value of the difference provides optimum agreement between their theoretical model and their wide range of kinetic experiments. Our best theoretical value [DZP CCSD(T) energies at DZP ROHF–CISD-optimized geometries] differs from Wagner's estimate by 7 kcal mol^{-1}. Possible reasons include the following. The theoretical method is apparently not adequate for the very different electronic structures involved, and thus the typical cancellation of errors is not present. Specifically, DZP is only a moderately large basis set, while CCSD(T) treats electron correlation highly accurately; therefore, the basis set size should be increased, and this should make up a large fraction of the discrepancy. Geometries may need to be optimized and ZPVEs evaluated at more reliable theoretical geometries. On the other hand, Walker and co-workers[7b] might argue that the assumed mechanism is incomplete, because it does not take into account a second route via the ^2A TS, nor does it consider possible reactions forming ethylene oxide (C_2H_4O) and OH from the intermediate hydroperoxyethyl radical CH_2CH_2OOH.[13]

(ii) Next consider the energy difference (or reaction enthalpy at 0 K) for $CH_3CH_2 + O_2 \rightarrow CH_3CH_2OO$ [s,g]. Theoretical values are –27.0, –28.0, –29.5, and –30.5 kcal mol^{-1} at the DZP CISD, CISD+Q, CCSD, and CCSD(T) levels of theory, to be compared with the value –32.9 kcal mol^{-1} of Wagner et al.[14] Wagner and co-workers obtained their value again from the above reaction mechanism and varying this reaction enthalpy as a parameter, but within a thermochemically determined range (from the equilibrium constants) of Slagle, Ratajczak, and Gutman.[10c] Another recent experimental work[42] gives for the reaction enthalpy

(42) (a) Dobis, O.; Benson, S. W. *J. Am. Chem. Soc.* **1993**, *115*, 8798. (b) Benson, S. W., private communication.

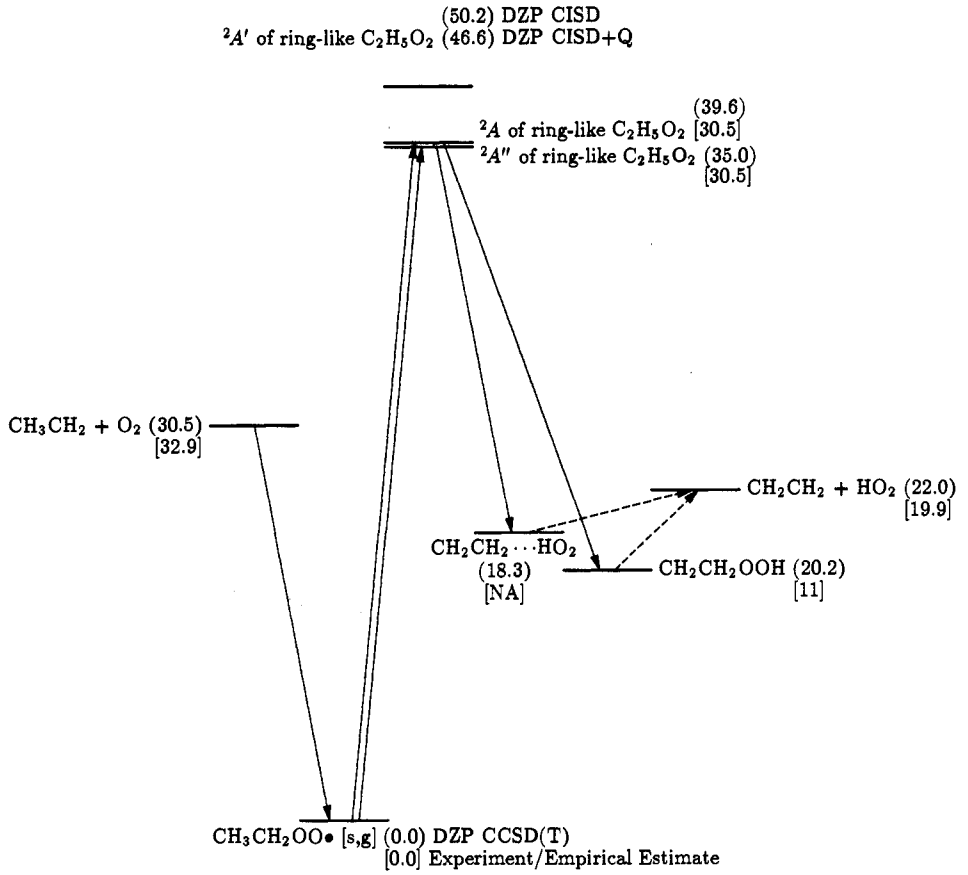

Figure 3. Schematic of the relative energies (kcal mol^{-1}) associated with the $CH_3CH_2 + O_2$ reaction.

at the room temperature, $\Delta H_{298}° = 31.4 \pm 0.5$ kcal mol^{-1}. As one can see, our best theoretical value differs from that of Wagner et al. by 2.4 kcal mol^{-1}, a considerable improvement with respect to comparison i, above.

(iii) Then consider the barrier height to internal hydrogen transfer, i.e., the energy difference between the transition states and CH_3CH_2OO [s,g]. Theoretical differences between $^2A''$ and [s,g] are 46.1, 41.3, 39.6, and 35.0 kcal mol^{-1} at the DZP CISD, CISD+Q, CCSD, and CCSD(T) levels. The comparable theoretical differences between ^2A and [s,g] are 46.4, 42.8, 41.1, and 39.6 kcal mol^{-1}. These are to be compared with the 34.3 ± 2.4 kcal mol^{-1} value of Baldwin, Pickering, and Walkter,[7b] the 31 kcal mol^{-1} value of Baldwin, Dean, and Walker,[11] and the 30.5 kcal mol^{-1} value of Wagner et al.[14] Skancke and Skancke[13] reported one TS belonging to C_1 symmetry and total energies and ZPVEs from which the barrier height may be extracted (among other things). These are 55.8, 42.5, 44.2, and 44.5 kcal mol^{-1} at the 6-31G* UHF, UMP2, UMP3, UMP4 levels of theory, respectively (all including ZPVEs at the 6-31G* UHF level and with optimized geometries at the same 6-31G* UHF level). One may argue that Skancke and Skancke's basis set 6-31G* is somewhat smaller than the DZP set, which has polarization functions on all hydrogen atoms, and that the treatment of electron correlation by UMPn (n = 2, 3, 4) is less complete than that by CCSD and CCSD(T); therefore, their best barrier height is 9.5 kcal mol^{-1} further from that of Wagner et al. than ours. Our best barrier (35.0 kcal mol^{-1}) differs from that of Wagner et al. (30.5 kcal mol^{-1}) by 4.5 kcal mol^{-1}, which is a considerable improvement from comparison i. This improvement may be largely attributed to cancellation of theoretical errors. The difference is larger than the above comparison ii, unexpectedly.

(iv) Wagner et al.[14] also estimated the reaction enthalpy for $CH_3CH_2 + O_2 \rightarrow CH_2CH_2OOH$ to be −21.9 kcal mol^{-1}. This differs from our best theoretical value [DZP CCSD(T) level] by 11.6 kcal mol^{-1}. The theoretical deficiencies mentioned in the above comparison i still exist, of course. But this large discrepancy between estimate and our best theoretical result is a strong indication that the estimate may have a considerable error.

(v) Finally, the reaction enthalpy for the overall reaction, $CH_3CH_2 + O_2 \rightarrow CH_2CH_2 + HO_2$, may be compared. The reaction enthalpy at room temperature, $\Delta H_{298}°$, is recommended by Baulch, Cobos, Cox, Esser, Frank, Just, Kerr, Pilling, Troe, Walker, and Warnatz[43] to be −13.0 kcal mol^{-1}. Our best theoretical value is −8.5 kcal mol^{-1}, resulting in a discrepany of 4.5 kcal mol^{-1}. This discrepany is not too large if, in addition to the above mentioned deficiencies in our theoretical methods, we keep in mind that the theoretical values here are for 0 K.

The enthalpy change for the reaction in question may also be determined from available standard heats of formation for the compounds involved. From Wagman, Evans, Parker, Schumm, Halow, Bailey, Churney, and Nuttall,[44] the relevant standard heats of formation are $\Delta H_f°_0(CH_3CH_2)$ = 119.2 kJ mol^{-1}, $\Delta H_f°_0(CH_2CH_2)$ = 60.731 kJ mol^{-1}, and $\Delta H_f°_0(HO_2)$ = 13.4 kJ mol^{-1}. Thus, the standard enthalpy change should be −45.1 kJ mol^{-1} or −10.8 kcal mol^{-1} at 0 K. This is in reasonable agreement with the chemical kinetical data from Baulch et al.[43] and in better agreement with our theoretical result.

At all levels of theory, the energy of the ^2A transition state is below that of the $^2A'$ stationary point (Hessian index 2) as expected, with the difference ranging from 3.8 (DZP CISD+Q) to 1.3 kcal mol^{-1} (DZ ROHF). Interestingly, the difference increases with basis set extension. Comparison of the two transition states ($^2A''$ and ^2A) shows that there is considerable difficulty describing the two systems to comparable accuracy with the methods used here. The energy differences $E(^2A) - E(^2A'')$ at various levels of theory, in a rough order of increasing

(43) Baulch, D. L.; Cobos, C. J.; Cox, R. A.; Esser, C.; Frank, P.; Just, Th.; Kerr, J. A.; Pilling, M. J.; Troe, J.; Walker, R. W.; Warnatz, J. *J. Phys. Chem. Ref. Data* **1992**, *21*, 411.

(44) Wagman, D. D.; Evans, W. H.; Parker, V. B.; Schumm, R. H.; Halow, I.; Bailey, S. M.; Churney, K. L.; Nuttall, R. L. *J. Phys. Chem. Ref. Data* **1982**, *11*, Suppl. 2.

sophistication, are 1.7, −1.8, 2.6, 4.3, 0.3, 1.5, 2.3, and 4.6 kcal mol^{-1} at the DZ ROHF, DZP ROHF, DZ CISD, DZ CISD+Q, DZP CISD, DZP CISD+Q, DZP CCSD, and DZP CCSD(T) levels, respectively.

The CH_2CH_2···HO_2 complex shows a remarkable consistency with respect to the products CH_2CH_2 + HO_2 and lends some confidence to the conclusion that this is a genuine minimum on the surface. The energy difference between the complex and the products varied between 1.9 kcal mol^{-1} at the DZ ROHF level to 3.2 kcal mol^{-1} at DZP CISD+Q. While the energy difference is not large, it is rather stable with respect to theoretical level.

Results for the products CH_2CH_2 + HO_2 (the intermediate ethylperoxy CH_3CH_2OO was discussed in paper 1) are more stable with respect to the level of theory than those for the transition-state systems. The energy difference increases with level of theory, and the increased sophistication helps the $^2A''$ [s,g] ethylperoxy more than the products CH_2CH_2 + HO_2, with the ringlike transition-state structure being helped most of all. The ΔH_r for reaction CH_3CH_2 + O_2 → CH_2CH_2 + HO_2 given in Table 3 is more sensitive to basis set than to the effects of electron correlation.

Turning finally to the higher level theoretical results in Table 4, the first thing to note is that the DZP CCSD(T) method is still a relatively inexact method for the transition states and that larger basis sets will be necessary for satisfactory accuracy. The experimental enthalpy of reaction ΔH_r for CH_3CH_2 + O_2 → CH_2CH_2 + HO_2 is within the estimated error of our work (±5 kcal mol^{-1}). Note that ZPVE corrections are included in the energies in Table 4. Our results for the transition states appear to be outside this error bar, although the CCSD(T) method gives a considerable improvement over CISD. The CCSD(T) method strongly favors the $^2A''$ state, even though the t_1 diagnostic indicates that the ^2A state has slightly more multireference character.

VI. Concluding Remarks

A study of the CH_3CH_2 + O_2 reaction mechanism has been carried out using state-of-the-art theoretical methods. Stationary points have been optimized (Figure 2) using extended basis sets and a selection of quantum mechanical methods that recover an increasing percentage of the correlation energy. The most important energetic results are summarized in Figure 3. The ringlike $C_2H_5O_2$ stationary point of $^2A''$ symmetry is predicted to be a true transition state, lying 35.0 kcal mol^{-1} above the intermediate CH_3CH_2OO. This activation energy is close to previous empirical estimates. A second transition state, incorporating no elements of point group symmetry, occurs much later along the reaction coordinate but lies less than 5 kcal mol^{-1} higher in energy. The possibility of two such transition states had not been suggested previously.

Acknowledgment. We would like to thank Dr. Albert F. Wagner (Argonne National Laboratory) for drawing our attention to the CH_3CH_2· + O_2 reaction in the course of two lectures at the Center for Computational Quantum Chemistry. We also thank Dr. Les Batt (University of Aberdeen, Scotland) and Dr. John H. Watson (University of London) for many helpful discussions. We also express appreciation to Professor Gustavo E. Scuseria (Rice University) for the open-shell CCSD and CCSD(T) computer programs used in this work. G.E.Q. would like to thank Professor Charles F. Jackels (Wake Forest University) and NASA for allowing an unpaid leave of absence for completion of this work. This research was supported by the U.S. Department of Energy, Office of Basic Energy Sciences, Division of Chemical Sciences, Fundamental Interactions Branch, Grant No. DE-FG09-87ER13811 and Contract No. DE-FC05-85ER2500000. Some computations reported here were performed at the IBM RS6000 serial cluster of the Cornell National Supercomputing Facility.

Supplementary Material Available: Tables A–K summarizing geometry and energy results, vibrational frequencies, and infrared intensity data for the structures investigated at the CISD and ROHF levels (12 pages). This material is contained in many libraries on microfiche, immediately follows this article in the microfilm version of the journal, and can be ordered from the ACS; see any current masthead page for ordering information.